Optical manipulation of micron/submicron sized particles and biomolecules through plasmonics

Xiaoyu Miao[1], Benjamin K. Wilson[1], Suzie H. Pun[2] and Lih Y. Lin[1,3]

[1]Department of Electrical Engineering, [2] Department of Bioengineering,
[3] Department of Physics, University of Washington, Seattle, WA 98195, USA
lin@ee.washington.edu

Abstract: Plasmonics, a rapidly emerging subdiscipline of nanophotonics, is aimed at exploiting surface plasmons for important applications, including sensing, waveguiding, and imaging. Parallel to these research efforts, technology yielding enhanced scattering and absorption of localized surface plasmons (LSPs) provides promising routes for trapping and manipulation of micro and nano scale particles, as well as biomolecules with low laser intensity due to high energy conversion efficiency under resonant excitation. In this paper, we show that the LSP-induced scattering field from a self-assembled gold nanoparticle array can be used to sustain trapping of single micron-sized particles with low laser intensity. Moreover, we demonstrate for the first time efficient localized concentration of sub-micron sized particles and DNAs of various sizes through photothermal effect of plasmonics.

OCIS codes: (240.6680) Surface plasmons; (350.4855) Optical manipulation.

References and links

1. C. E. Talley, J. B. Jackson, C. Oubre, N. K. Grady, C. W. Hollars, S. M. Lane, T. R. Huser, P. Nordlander, and N. J. Halas, "Surface-enhanced Raman scattering from individual Au nanoparticles and nanoparticle dimer substrates," Nano. Lett. **5**, 1569-1574 (2002).
2. P. Anger, P. Bharadwaj, and L. Novotny, "Enhancement and quenching of single-molecule fluorescence," Phys. Rev. Lett. **96**, 113002-1 – 113002-4 (2006).
3. I. H. El-Sayed, X. Huang, and M. A. El-Sayed, "Surface plasmon scattering and absorption of anti-EGFR antibody conjugated gold nanoparticles in cancer diagnostics: applications in oral cancer," Nano. Lett. **5**, 829-834 (2005).
4. C. Loo, A. Lowery, N. J. Halas, J. L. West, and R. Drezek, "Immunotargeted nanoshells for integrated cancer imaging and therapy," Nano. Lett. **5**, 709-711 (2005).
5. S. R. Sershen, S. L. Westcott, N. S. Halas, and J. L. West, "Temperature-sensitive polymer-nanoshell composites for photothermally modulated drug delivery," J. Biomed. Mater. Res. **51**, 293-298 (2000).
6. D. A. Boyd, L. Greengard, L. Brongersma, M. Y. El-Naggar, and D. G. Goodwin, "Plasmon-assisted chemical vapor deposition," Nano. Lett. **6**, 2592-2597 (2006).
7. G. L. Liu, J. Kim, Y. Lu, and L. Lee, "Optofluidic control using photothermal nanoparticles," Nat. Mat. **5**, 27-32 (2005).
8. X. Miao, B. K. Wilson, and L. Y. Lin, "Localized surface plasmon assisted microfluidic mixing," App. Phys. Lett. **92**, 124108-1 – 124108-3 (2008).
9. A. Ashkin, "Acceleration and trapping of particles by radiation pressure," Phys. Rev. Lett. **24**, 156-159 (1970).
10. A. Ashkin, "Optical trapping and manipulation of neutral particles using lasers," Proc. Natl. Acad. Sci. USA, **94**, 4853-4860 (1997).
11. L. Novotny, R. X. Bian, and S. Xie, "Theory of nanometric optical tweezers," Phys. Rev. Lett. **79**, 645-649 (1997).
12. P. C. Chaumet, A. Rahmani, and M. Nieto-Vesperinas, "Optical trapping and manipulation of nano-objects with an apertureless probe," Phys. Rev. Lett. **88**, 123601-1 – 123601-4 (2002).
13. M. Righini, A. S. Zelenina, C. Girard, and R. Quidant, "Parallel and selective trapping in a patterned plasmonic landscape," Nat. Phys. **3**, 477-480 (2007).
14. A. N. Grigorenko, N. W. Roberts, M. R. Dickinson, and Y. Zhang, "Nanometric optical tweezers based on nanostructured substrates," Nat. Photo. **2**, 365-370 (2008).

#98225 - $15.00 USD Received 7 Jul 2008; revised 10 Aug 2008; accepted 12 Aug 2008; published 18 Aug 2008

15. M. Righini, G. Volpe, C. Girard, D. Petrov, and R. Quidant, "Surface plasmon optical tweezers: tunable optical manipulation in the femtonewton range," Phys. Rev. Lett. **100**, 186804-1 – 186804-4 (2008).
16. X. Miao, B. K. Wilson, G. Cao, S. H. Pun, and L. Y. Lin, "Long-range trapping and rotation of nanowires by plasmonic tweezers," Submitted to Nano Lett.
17. D. Braun and A. Libchaber, "Trapping of DNA by thermophoretic depletion and convection," Phys. Rev. Lett. **89**, 188103-1 – 188103-4 (2002).
18. V. Garcés-Chávez, R. Quidant, P. J. Reece, G. Badenes, L. Torner, and K. Dholakia, "Extended organization of colloidal microparticles by surface plasmon polariton excitation," Phys. Rev. B **73**, 085417-1 – 085417-5 (2006).
19. X. Miao and L. Y. Lin, "Large dielectrophoresis force and torque induced by localized surface plasmon resonance of a cap-shaped Au nanoparticle array," Opt. Lett. **32**, 295-297 (2007).
20. E. L. Hinrichsen, J. Feder, and T. Jøssang, "Geometry of random sequential adsorption," J. Stat. Phys. **44**, 793-827 (1986).
21. X. Miao and L. Y. Lin, "Trapping and manipulation of biological particles through a plasmonic platform," IEEE J. Sel. Top. Quantum. Electron. **13**, 1655-1661 (2007).
22. H. Xu and M. Käll, "Surface plasmon enhanced optical forces in silver nanoaggregates," Phys. Rev. Lett. **89**, 246802-1 – 246802-4 (2002).

Localized surface plasmons are collective electron oscillations confined in metallic nanostructures generated by an external electric field excitation in the form of light. The motion of the confined electrons inside the nanostructures can be modeled as a damped harmonic oscillator driven by the external force. The building surface charges act as an effective restoring force, allowing a resonance to occur at a specific frequency when the response of electrons shows a $\pi/2$ phase lag with respect to the driving field. At resonance, the electron oscillations inside the nanostructure lead to enhanced scattering and absorption cross sections. The enhanced scattering field of metallic nanostructures has been utilized in applications such as surface enhanced Raman spectroscopy (SERS)[1], fluorescence enhancement and quenching[2], and contrast agents for biomedical imaging[3]. At the same time, the enhanced absorption of metallic nanostructures (photothermal effect) is also found to be useful for cancer therapy[4], controlled drug delivery[5], chemical vapor deposition[6], and guiding[7] and mixing[8] of micro-fluidic flow.

Manipulation of single particles and particle ensembles using optical approaches has been an active research topic since the invention of optical tweezers by Ashkin in the early 1970s[9]. Optical tweezers make use of the optical gradient force in a highly focused laser beam to trap the particle at the beam focus. This technique has already been applied to a diverse variety of particles including atoms, molecules, dielectric spheres, with sizes ranging from tens of nanometers to tens of micrometers, as well as biological particles such as virus, cells and cellular organelles[10]. However, optical tweezers directly convert optical energy into mechanical energy, which is an inefficient process and requires a tightly focused intense laser beam to achieve significant force. Enhancement and confinement of surface plasmon field have been theoretically predicted to have important applications in trapping of micro and nano particles with lower optical intensity[11-12]. Recently, parallel and selective trapping of micron-sized particles using ordered gold patterns have been reported[13]. Nanometric optical tweezers with sub-diffraction-limited trapping volume have been realized by utilizing optical near field between gold nanodots fabricated by electron beam lithography[14,15]. A unique long-range trapping phenomenon of vanadium dioxide (VO_2) nanowires on a self-assembled plasmonic substrate instigated at a distance from the focused laser source has also been observed[16].

In addition to forming the enhanced optical field, the LSP energy also dissipates through a non-radiative process and is transferred into heat, producing a localized heat source and temperature gradient in the adjacent medium. In general, temperature gradients in a fluidic environment are known to induce both convective flow and thermophoresis. The convective flow drives the liquid out from the region around the heat source and pulls in cooler liquid in order to transfer heat to the surrounding medium. Under a temperature gradient particles suspended in the liquid are also driven toward the cold region by thermal diffusion, a process known as thermophoresis. A previous study shows that the interplay of convection and

#98225 - $15.00 USD Received 7 Jul 2008; revised 10 Aug 2008; accepted 12 Aug 2008; published 18 Aug 2008

thermophoresis provides a concentration mechanism for macromolecules such as DNA under direct infrared laser excitation[17]. More recently, a large scale organization of colloidal particles was demonstrated by surface plasmon polariton excitation, where the enhanced optical force, thermophoretic and convective force are shown to dominate under different conditions and lead to different particle dynamics[18].

In this paper, we demonstrate that both the LSP-induced enhanced scattering and absorption can be harnessed for manipulation of micron and submicron sized particles. We describe the laser intensity threshold to sustain trapping of single micron-sized dielectric spheres by the enhanced scattering field. We also show that the photothermal effect of the same plasmonic substrate can be utilized to concentrate sub-micron dielectric particles, DNA of various sizes.

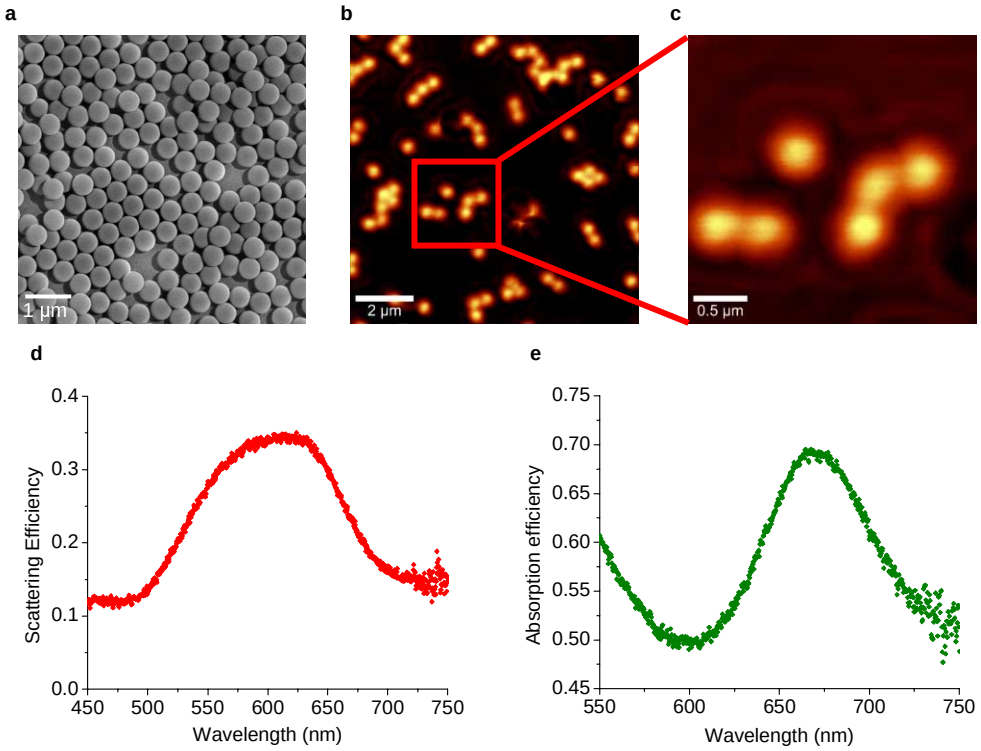

Fig. 1. (a) SEM micrograph of the self-assembled gold nanoparticles. The diameter of individual gold nanoparticles is about 450 nm. (b) NSOM image of the plasmonic substrate where the nanoparticle distribution is sparse, showing the near-field radiation. The wavelength of the excitation laser is 633 nm. (c) High magnification view of the area marked with the red square in (b). (d) Scattering efficiency spectrum of the plasmonic substrate, showing the peak at 624 nm. (e) Absorption efficiency spectrum of the plasmonic substrate, showing the peak at 668 nm.

In our experiment, a close-packed gold nanoparticle array fabricated on a glass coverslip through self assembly[19] functions as the plasmonic substrate. Before carrying out the trapping experiment, the plasmonic substrate is characterized using scanning electron microscopy (SEM), near-field scanning optical microscopy (NSOM) and UV/VIS spectroscopy. The scanning electron micrograph of the plasmonic substrate in Fig. 1(a) shows a random distribution of the self-assembled gold nanoparticles, where the jamming coverage is estimated to be about 53.4%, which is close to the theoretical upper limit of 54.7% of random sequential adsorption[20]. The NSOM images shown in Fig. 1(b) and (c), obtained by WiTec Alpha300S, were specifically taken in the region where the nanoparticle distribution is sparse

#98225 - $15.00 USD Received 7 Jul 2008; revised 10 Aug 2008; accepted 12 Aug 2008; published 18 Aug 2008

under 633-nm excitation, in order to show the radiation patterns from individual nanoparticles. The near-field radiation shows clear resonance, which cannot be seen if excited under a non-resonant wavelength, e.g., 532 nm. The scattering and absorption efficiency spectra of the nanoparticle array characterized by a UV/VIS spectrometer (Newport) are shown in Fig. 1(d) and (e), respectively. The efficiency on y-axis represents the percentage of incident light scattered/absorbed by the nanoparticle array. The spectra show that about 34% and 56% of the incident light energy is dissipated through plasmon scattering and absorption at the excitation laser wavelength (633 nm), respectively, given the gold nanoparticle coverage shown in Fig. 1(a). Such high energy conversion efficiencies are the key to realizing trapping of micro and nano particles with a low optical intensity.

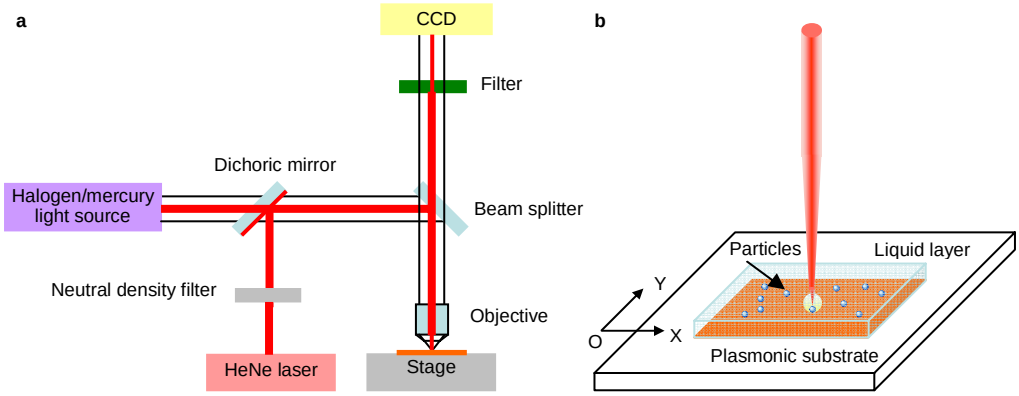

Fig. 2. (a) Experimental setup for the trapping and concentration experiments on the plasmonic substrate. (b) Detailed configuration of the sample chamber.

The experimental configuration for the described work is depicted in Fig. 2. A fluorescence upright microscope (Zeiss Axio Imager) is adopted as the platform for observation of particle motions. A sample chamber with a thickness about 1 mm is built upon the plasmonic substrate by a spacer structure. The top of the chamber is covered by a standard glass coverslip (VMR Labshop). The liquid solution containing polystyrene beads or DNA can be introduced to the chamber through a pipette. The whole chamber is placed on the programmable motorized stage (Ludl, BioPrecison) of the microscope. A HeNe laser (Research Electro-Optics) with wavelength at 633 nm and full power of 25 mW is directed into the optical path of the microscope by a customized dichroic mirror (Chroma) and focused by a long working distance microscopic objective lens with low numerical apertures (Zeiss, 20×, NA = 0.22 or 50×, NA = 0.45). The laser power delivered to the plasmonic substrate can be modulated by a continuously variable metallic neutral density filter (Thorlabs). The focal plane of the microscope is adjusted to the surface of the plasmonic substrate, and the particles that can be observed under the microscope are also close to this focal plane. The images are acquired by a high-speed charge-coupled device (CCD) camera (Zeiss, AxioCam). The fluorescent intensities are analyzed by MATLAB (Mathworks) processing the CCD images.

Single particle trapping can be clearly visualized under the microscope after the laser is turned on and LSPs are activated on the plasmonic substrate. As reported in previous theoretical study[21], the maximum of the scattering field from the random gold nanoparticle array will occur at the center of the laser spot on the array. Therefore, a micron-sized particle will be trapped at the center of the nanoparticle array area illuminated by the laser due to the optical gradient force. This has been demonstrated experimentally for single micron-sized polystyrene beads[19] or biological cells[21]. By continuously increasing the laser power delivered to the plasmonic substrate, a convective fluidic flow can be eventually formed to dissipate the thermal energy into the surrounding medium when the induced temperature gradient due to photothermal effect exceeds a threshold. We find that the convective flow provides an

#98225 - $15.00 USD Received 7 Jul 2008; revised 10 Aug 2008; accepted 12 Aug 2008; published 18 Aug 2008

efficient way to achieve light-induced concentration of particles with various sizes including biomolecules such as DNAs.

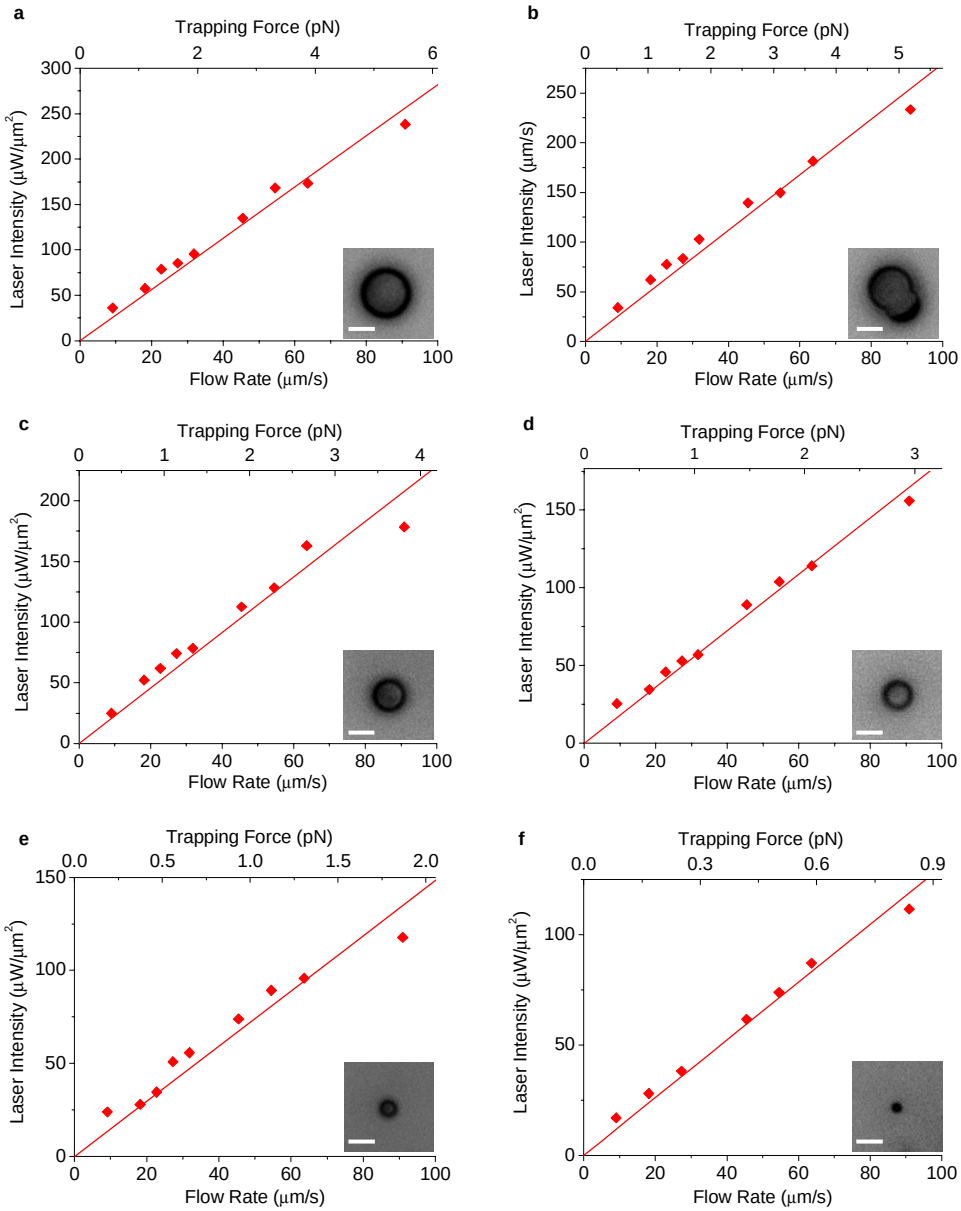

Fig. 3. The minimum laser intensity to maintain the trap as a function of flow rate of surrounding fluid utilizing plasmonic trapping. All the optical intensities are measured at the sample plane under the microscope objective. (a) – (f) show the measurement results for single polystyrene beads with diameter 7.3, 6.3 (non-spherical), 5.0, 3.9, 2.5 and 1.1 μm, respectively. The insets show the corresponding microscopic images of particles. The scale bars in all images represent 5 μm in length.

We first quantitatively study the trapping of individual micron sized particles through the plasmonic scattering field when the laser intensity is below the threshold of inducing the thermal convective flow. We measure the minimum laser intensity required to achieve the corresponding amount of trapping force, which is proportional to the flow rate of the

#98225 - $15.00 USD Received 7 Jul 2008; revised 10 Aug 2008; accepted 12 Aug 2008; published 18 Aug 2008

surrounding fluid relative to the trapped particle. By programming the motorized stage, the flow rate of the surrounding fluid can be discretely adjusted from 0 to 100 μm/s. Figure 3(a-f) shows the measured optical intensity threshold as a function of flow rate or trapping force for polystyrene beads (Polysciences) with various sizes. The results in Fig. 3(f) show that optical intensity as low as 17 μW/μm^2 can maintain the trapping of 1.1-μm bead, when the flow rate of the surrounding fluid is 9 μm/s. This intensity is a few orders lower than the minimum intensity required in conventional optical tweezers setup with a tightly focused laser beam (on the order of 10^3 μW/μm^2), and also lower than the values recently reported using lithographically patterned plasmonic structures for trapping (50 μW/μm^2 in [13] and > 150 mW focused into diffraction limit in [14]). Fig. 3 also shows that the measured laser intensity threshold is approximately linear related to the flow rate, as expected from the theoretical analysis below. Moreover, the slope of the fitted line (ratio between the optical intensity threshold and flow rate) in Fig. 3 has an approximately linear relationship with particle size as shown in Fig. 4, indicating the advantage of plasmonic trapping especially for smaller particles.

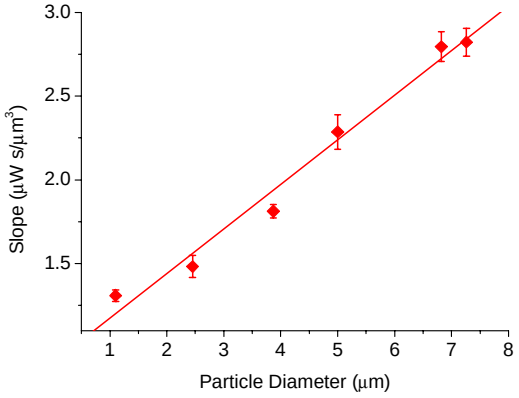

Fig. 4. The slope of the fitted line through origin in Fig. 3 versus particle size for plasmonic trapping. The error bars show the standard deviations of the linear fits.

By making approximation that the plasmonic scattering field follows a simple dipolar radiation pattern, the scattering field is inversely proportional to the radial distance from the radiation source in the far-field regime (micron-sized particle used in the experiment is only influenced by the scattering far field). The optical trapping force induced by the gradient of this scattering field can be described by,

$$F_{trap} = \frac{Ka^3 P}{r^3} \tag{1}$$

where K is a constant, a is the radius of the polystyrene bead, P is the laser power, and r is the center-to-center distance from the radiation source to particle[22]. At the optical intensity threshold, the trapping force is considered to be equal to the viscous drag force described by the Stokes equation,

$$F_{drag} = 6\pi\eta a V \tag{2}$$

where η and V is the viscosity and flow rate of fluid, respectively. Linking Eq. (1) and (2) gives $\partial P / \partial V \propto a$, assuming $r \approx a$ when the particle is trapped on the surface of the plasmonic substrate. This simplified theoretical analysis is well consistent with the experimental results, and confirms the trapping mechanism through plasmonic scattering field.

As the laser intensity at the sample plane continues to increase, a thermally induced convective flow is observed eventually. The LSPs are confined to the surface of gold nanoparticle array which acts as a localized heat source. When temperature gradients along

#98225 - $15.00 USD Received 7 Jul 2008; revised 10 Aug 2008; accepted 12 Aug 2008; published 18 Aug 2008

the depth direction are induced in the microfluidic environment and exceed a certain threshold, convective flow is formed to circulate fluid around in order to transfer heat from the localized heat source to the surrounding colder regions. The fluid from the surrounding regions is drawn toward the heat source and then upward. The particles in the fluid initially move with the fluidic flow towards the center of the laser spot. Once the laser is turned off, the convective flow attenuates and the particles eventually accumulate at the location of heat source defined by the laser spot.

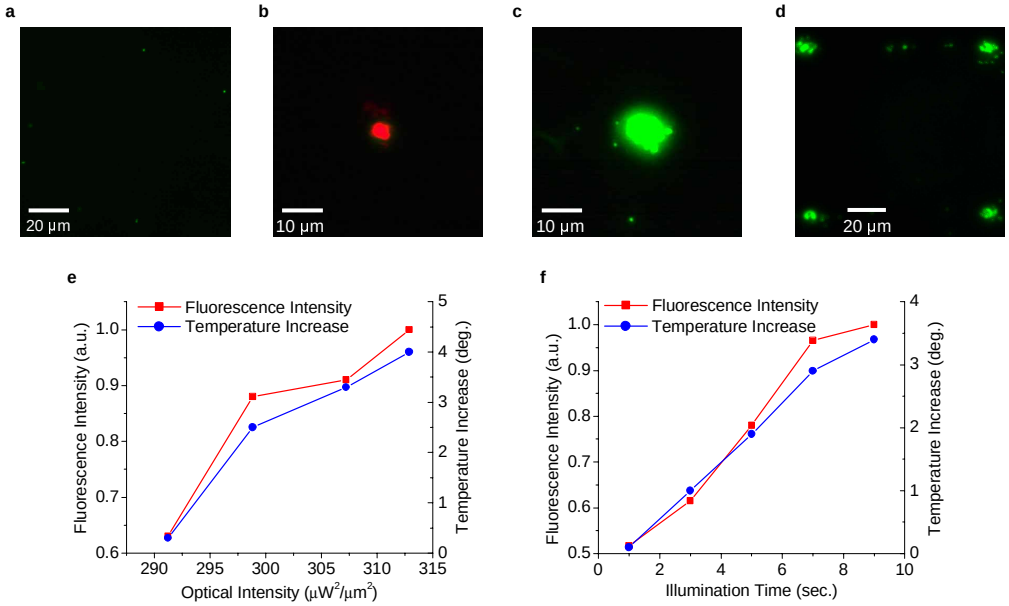

Fig. 5. (Media 1) Optical images of (a) fluorescent polystyrene beads with 590-nm diameter randomly distribute in the liquid. (b) The laser spot on the gold nanoparticle array. The diameter of the laser spot is estimated to be about 5 μm. (c) A strong localized concentration of sub-micron sized polystyrene beads at the same location of the laser spot. The snapshot shown in (c) is taken with the same domain as that in (b). (d) The sub-micron sized polystyrene beads are concentrated at the four corners of the domain in (a). (e) Average fluorescence intensity and temperature increase of the concentration site as a function of laser intensity. The illumination time is kept the same for all the measurements in (e). (f) Average fluorescence intensity and temperature increase of the concentration site as a function of illumination time. The laser illumination intensity is kept the same for all the measurements in (f). The fluorescence intensities of concentrated particles shown on left y-axis in (e) and (f) have been normalized to the maximum in (e) and (f), respectively.

The threshold value of laser intensity to induce the convective flow varies with location of the focused spot. This is because the gold nanoparticles are randomly distributed on the substrate and the density is not uniform. We first conducted the measurement at 50 different locations on the plasmonic substrate which were randomly chosen. The average value of the laser intensity threshold measured at the sample plane is 256.9 $\mu W/\mu m^2$ and the standard deviation is 26.3 $\mu W/\mu m^2$. For demonstration of convective flow-induced concentration, fluorescent polystyrene beads with a diameter of 590 nm ($\lambda_{emission}$ = 520 nm, Bangs Laboratories) are used. Before turning on the laser, the sub-micron sized polystyrene beads are observed to randomly distribute in the liquid (Fig. 5(a)) and undergo strong Brownian motions. When the laser is turned on with the intensity exceeding the threshold, the thermal convective flow is observed to form without noticeable delay (see supplemental video information). After the laser is turned off, the fluorescent polystyrene beads are found to accumulate at the location of the laser spot. Although intuitively the particles should diffuse away over a time scale of seconds because of the Brownian motion, our experiment shows that once the particles are concentrated, they remain stable at the location even after an hour,

#98225 - $15.00 USD Received 7 Jul 2008; revised 10 Aug 2008; accepted 12 Aug 2008; published 18 Aug 2008

possibly due to a surface adsorption process. Figure 5(b) and (c) show the laser spot and concentrated fluorescent beads, respectively. A few particles are observed to locate outside the heat source region after the accumulation occurs. This effect is likely due to the thermophoretic force, which drives particles toward cold region from heat source radially. Enhanced optical radiation force associated with the scattering electric field from LSPs is also involved in this process, which has been theoretically suggested to trap the particle at junctions between closely spaced metal nanoparticles (hot spots)[22]. By changing the location of laser spot, we are able to define the specific sites where submicron sized particles are concentrated and form a pattern shown in Fig. 5(d). Figure 5(e) and (f) show that the concentration increases with either increasing laser intensity or illumination time, due to higher generated heat which induces a stronger convective flow and therefore more particles to be concentrated.

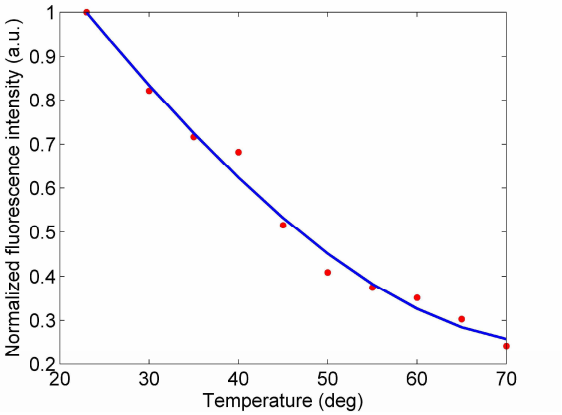

Fig. 6. Calibration curve of fluorescence intensity of Rhodamine B used for temperature measurement, where red dots are data points measured in the experiment and blue curve is the fitted line.

When the photothermally induced concentration approach is applied to biological particles, it becomes important to characterize the temperature increase, which is a potential concern for stability and integrity of biological particles. To study this, a temperature-sensitive dye Rhodamine B is used to measure the temperature increase due to non-radiative relaxation of LSPs. Figure 6 shows the calibration curve of fluorescence intensity of Rhodamine B versus temperature. The intensity was measured as an average within the focused laser spot, with the imaging plane focused at the Au nanoparticle array surface. The results in Fig. 5(e) and (f) indicate that the temperature increase is less than 4 degrees with the laser intensity and illumination time used in our experiment.

To show that convective flow-induced concentration is also applicable to biomolecules, we performed similar experiments on large molecular weight DNA and oligonucleotides. Lambda DNA (8.4 Kbp, New England BioLabs) is stained with POPO-1 ($\lambda_{emission}$ = 456 nm, Invitrogen) in a TAE (Tris-Acetate) buffer. The oligonucleotide (5'biotin-GAG-CTG-CAC-GCT-GCC-GTC-3', Integrated DNA Technologies) is linked to streptavidin modified quantum dots ($\lambda_{emission}$ = 525 nm, Invitrogen) in a PBS (Phosphate Buffered Saline) buffer. Figure 7(a) and (b) show the snapshots of DNA fluorescence before and after the laser excitation on plasmonic substrate, respectively. These two snapshots are taken in the same domain and with the same exposure time. Figure 7(c) quantitatively shows the distributions of fluorescence intensity along the vertical bisector of Fig. 7(a) and (b), which clearly illustrates the concentration effect. Notice that the DNA fluorescence intensity is reduced in regions outside the trapping site. This is attributed to the photobleaching process of the fluorescence dye, which sustains chemical damage such as oxidation. Figure 7(d) and (e) show the snapshots of oligonucleotides fluorescence before and after the laser excitation on plasmonic

#98225 - $15.00 USD Received 7 Jul 2008; revised 10 Aug 2008; accepted 12 Aug 2008; published 18 Aug 2008

substrate, respectively. Similar concentration effect is visualized in Fig. 7(f), which plots the distribution of fluorescence intensity along the vertical bisector of Fig. 7(d) and (e). The ring geometry of the fluorescence from the concentrated oligonucleotides shows that the thermophoretic repulsion is significant in this process, which depletes the accumulated oligonucleotides in the center. The observed ring geometry is consistent with the result reported by Braun et al[17], where they showed the depletion and convection of plasmid-sized DNA by infrared laser heating. Figure 7(f) also shows that the fluorescence intensity of oligonucleotides outside the concentration site stays about the same before and after the trapping process, as the quantum dots are inorganic materials which have a much slower photobleaching rate compared to organic fluorescence dye.

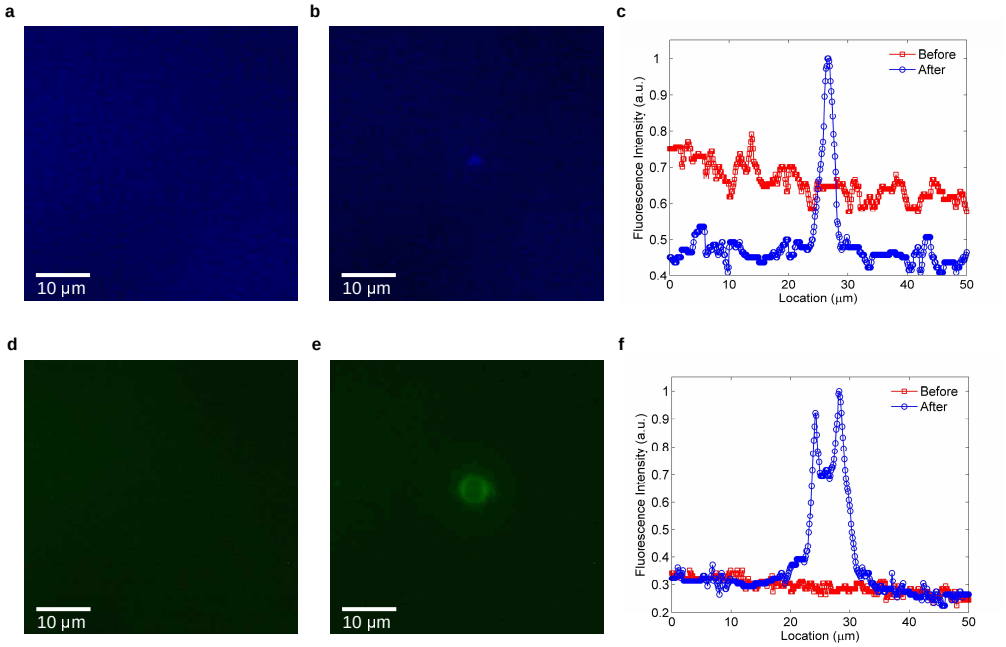

Fig. 7. Fluorescence images of λ DNA stained by POPO-1 (a) before and (b) after the laser illumination. (c) Fluorescence intensity profile along the vertical bisectors in (a) and (b), showing the concentration of λ DNA by surface plasmon-induced thermal convective flow. Fluorescence images of quantum dot-labeled oligonucleotides (d) before and (e) after the laser illumination. (f) Fluorescence intensity profile along the vertical bisectors in (d) and (e), showing the trapping of oligonucleotides by surface plasmon-induced thermal convective flow.

To conclude, we have demonstrated that both the enhanced scattering and absorption from a plasmonic substrate can be utilized for trapping of micro and submicron scale particles. The enhanced scattering field supports the trapping of single micron-sized particles with higher efficiency compared to conventional optical tweezers. The demonstrated laser intensity for trapping is also lower than other reported using plasmonic trapping approaches. At the same time, the enhanced absorption of the plasmonic substrate can be utilized to achieve localized thermo-optic concentration of sub-micron particles and DNA. Both approaches require relatively low optical intensity due to high energy conversion efficiency through plasmonics. Future work will address optimization of the plasmonic substrate, which will be specifically designed for scattering or absorption-based trapping applications.

Acknowledgment

This work is supported by the National Science Foundation under Grant DBI 0454324 and by the National Institute of Health under Grant R21 EB005183. We thank WiTec for their help in obtaining the NSOM image.

#98225 - $15.00 USD Received 7 Jul 2008; revised 10 Aug 2008; accepted 12 Aug 2008; published 18 Aug 2008